

DESIGN OF A NOVEL OPTIMAL CONTROL ENERGY MANAGEMENT STRATEGY FOR STAND ALONE HYBRID SOLAR-WIND SYSTEM

Abhishek Singh Chauhan, Deepak Kumar Joshi, Nirma Kumari Sharma

E-Mail Id: abhisheksinghchauhan2112@gmail.com

Department of Electrical Engineering, Mewar University, Chittorgarh, Rajasthan, India

Abstract- Energy is pivotal for the economic progress and societal advancement of any nation. To minimize reliance on imported fuels and address the increasing gap between energy demand and supply, it is imperative to optimize indigenous energy resources, while considering economic, environmental, and social constraints. The surge in population has exacerbated the energy crisis, widening the disparity between demand and supply. Depletion of conventional energy sources has led to an energy supply shortfall. While renewable energy sources (RES) offer promise in the energy sector, their standalone operation is hindered by their intermittent nature, resulting in interruptions in power supply to loads. To ensure stable and reliable power supply, hybrid combinations of renewable energy sources have been adopted. The design of a hybrid wind-solar Photovoltaic (SPV) system for power generation, targeting domestic households in remote areas disconnected from the grid, has been proposed. Such hybrid systems operate either in isolated mode or in grid-connected mode via power electronics interfaces, augmenting reliability and ensuring continuous power supply. Introducing a Hybrid Renewable Energy System (HRES) aims to enhance the productivity and operability of individual renewable energy systems. Extensive technological investigations have explored various approaches, including linear programming and a novel optimum control strategy incorporating PID controllers, fuzzy logic controllers, AI, and optimal torque with Maximum Power Point Tracking (MPPT) techniques. The developed novel optimum control strategy facilitates the coordinated operation of diverse devices and power interface circuitries, with the primary objective of ensuring continuous power supply. Simulation studies have evaluated system performance under different scenarios, including varying solar radiation, temperature, air conditions, and battery charge/discharge conditions. Results indicate variable power generation and affirm the efficacy of the integrated system and control strategies in real-time installations. The investigation reveals that the developed novel optimum control strategy significantly enhances the performance of standalone hybrid wind-SPV systems. The hybrid system, when integrated with controllers, exhibits improved output power and ensures continuous power delivery, thereby enhancing overall system efficiency and reliability. Such systems are indispensable in isolated regions where grid connectivity is unavailable, ensuring secure power generation by intelligently harnessing diverse energy sources.

Keywords: PV, WECS, ESS, ANN, FLC, EMS, HRES.

1. INTRODUCTION

With fossil fuel depletion and increasing atmospheric pollution, there's a growing interest in renewable energy sources like PV, wind, and hydro. Solar and wind energy are abundant worldwide, yet their fluctuating nature leads to intermittent power generation. To address this, Hybrid Renewable Energy Systems (HRES) combine multiple energy sources with storage systems, offering greater efficiency and lower energy production costs compared to single-source systems. Effective management of HRES energy is crucial due to the variability in generated power. Existing literature introduces various HRES configurations operating in grid-connected or standalone modes. Energy management in HRES often employs PI controllers to regulate buck-boost bidirectional converters for battery charging/discharging and implement current control strategies for power balance. However, conventional control strategies rely heavily on mathematical system modeling. Hybrid systems emerge as a viable solution for remote or micro-generation units connected to weak AC grids, combining conventional and renewable energy sources via a DC bus. In isolated areas, integrating electro-chemical storage with hybrid systems eliminates the need for diesel generators. This study focuses on a hybrid generation system integrating PV, wind turbines, and storage batteries to address periods of low generation and implement system control. Various hybrid system topologies exist, differing in interface converters between sources and interconnection techniques. This system topology emphasizes maximum energy transfer, involving investigation into energy losses, power conditioning converters, optimal control, and energy management. The primary objective of this study is to explore hybrid system configuration, dynamic modeling, energy management, and control strategies. The author proposes and evaluates an efficient control strategy for managing energy in a standalone hybrid solar-wind system under diverse operating conditions. Given the continuous energy demand, battery backups are integrated into the hybrid system, ensuring efficiency under varying weather and load conditions.

2. PROPOSED CONFIGURATION AND MODELING OF THE HRES

The proposed standalone hybrid renewable energy-based power system integrates solar PV, wind, and battery systems. Figure 1 illustrates the Simulink block diagram of the proposed hybrid standalone system. Coordinating and controlling the output from various generation sources in a hybrid system is essential to fully realize their benefits. Given the complexity of power management, control, and operation in hybrid systems compared to individual systems, effective control strategies are vital to ensure system sustainability to the maximum extent.

Solar panels generate DC power, which fluctuates due to variable irradiation levels caused by seasonal weather conditions. To stabilize power output, a boost converter is employed to provide constant power for the DC link, maintaining power at a consistent level. Wind panels generate AC power through rotating wind turbines, with wind variability being a characteristic feature. However, the panel power is converted to DC through an AC to DC converter to interface with the DC bus, which connects the generator to the load. Batteries store DC power, necessitating a bidirectional boost converter for constant power storage. This converter facilitates the efficient transfer of power to and from the battery, ensuring stable energy storage and retrieval within the system.

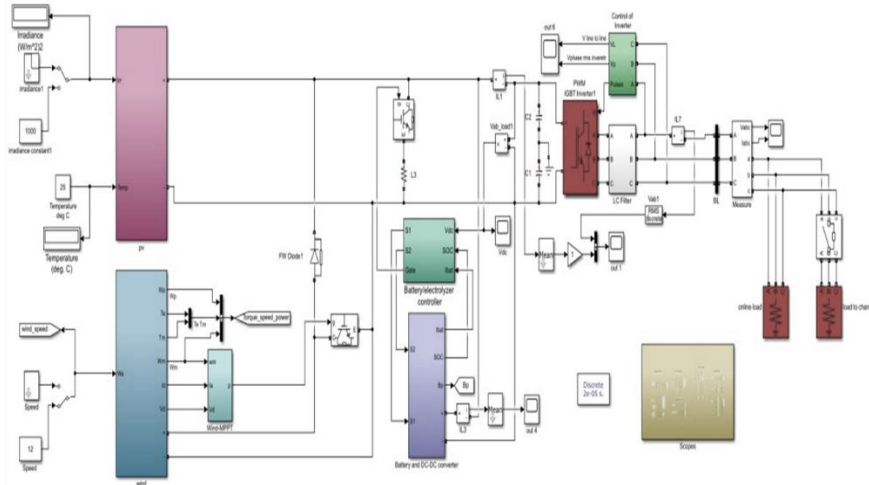


Fig. 2.1 MATLAB/Simulink Implementation of Dynamic Model for Hybrid Solar PV Wind Microgrid

2.1 PV System Modeling

The equivalent circuit of a PV cell is shown in Fig. 2.1. The current source I_{ph} represents the cell photocurrent. R_{sh} and R_s are the intrinsic shunt and series resistances of the cell, respectively. Usually the value of R_{sh} is very large and that of R_s is very small, hence they may be neglected to simplify the analysis. Practically, PV cells are grouped in larger units called PV modules and these modules are connected in series or parallel to create PV arrays which are used to generate electricity in PV generation systems. The equivalent circuit for PV array is shown in Fig. 2.2.

The voltage-current characteristic equation of a solar cell is provided:

$$\text{Module photo-current } I_{ph}: I_{ph} = [I_{sc} + K_i (T - 298)] * I_r / 1000$$

Here: I_{ph} : photo-current (A), I_{sc} : short circuit current (A), K_i : short-circuit current of cell at 25 °C and 1000 W/m², T: operating temperature (K), I_r : solar irradiation (W/m²).

$$\text{Module reverse saturation current } I_{rs}: I_{rs} = I_{sc} / [\exp (qV_{oc} / N_s kT) - 1]$$

Here: q: electron charge = 1.6×10^{-19} C, V_{oc} : open circuit voltage (V), N_s : number of cells connected in series, n: the ideality factor of the diode, k: Boltzmann's constant, = 1.3805×10^{-23} J/K.

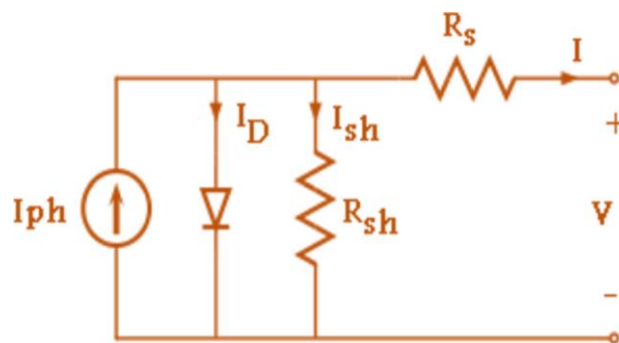
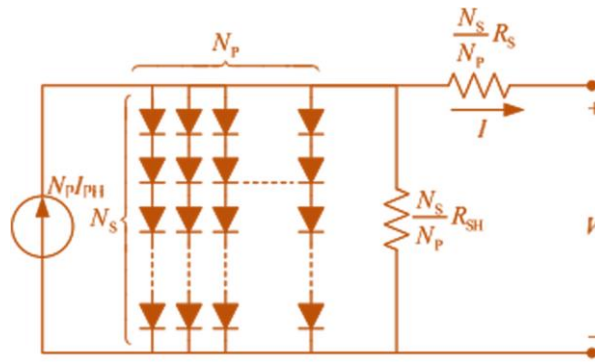


Fig. 2.1 PV Cell Equivalent Circuit


Fig. 2.2 Equivalent Circuit of Solar Array

The module saturation current I_0 varies with the cell temperature, which is given by:

$$I_0 = I_{rs} \left[\frac{T}{T_r} \right]^3 \exp \left[\frac{q \times E_{g0}}{nk} \left(\frac{1}{T} - \frac{1}{T_r} \right) \right] \quad (1)$$

Here: T_r : nominal temperature = 298.15 K, E_{g0} : band gap energy of the semiconductor = 1.1 eV The current output of PV module is:

$$I = N_p \times I_{ph} - N_p \times I_0 \times \left[\exp \left(\frac{V/N_s + I \times R_s/N_p}{n \times V_t} \right) - 1 \right] - I_{sh} \quad (2)$$

$$\text{With } V_t = \frac{k \times T}{q} \text{ and } I_{sh} = \frac{V \times N_p / N_s + I \times R_s}{R_{sh}}$$

Here: N_p : number of PV modules connected in parallel, R_s : series resistance (Ω), R_{sh} : shunt resistance (Ω), V_t : diode thermal voltage (V).

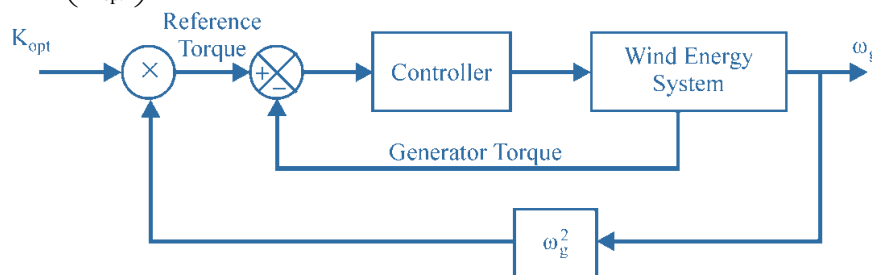
2.2 Wind System Modeling

The torque controller aims to enhance the efficiency of wind energy capture across a broad spectrum of wind speeds by ensuring the generated power remains at its optimum level. This is achieved through the block diagram depicted in Figure 2.3. Irrespective of the wind velocity, the Maximum Power Point Tracking (MPPT) tool imposes a torque reference capable of extracting the maximum available power. The curve T_{opt} is represented as:

$$T_{opt} = K_{opt} * \omega_{opt}^2 \quad (3)$$

Where

$$K_{opt} = 0.5 * \rho * A * \left(\frac{r_m}{\lambda_{opt}} \right)^3 * C_{P-max} \quad (4)$$


Fig. 2.3 optimal torque control MPPT method

The PMSG model is presented in figure. This dynamic model assumes no saturation, a sinusoidal back e.m.f. and negligible eddy current and hysteresis losses. It takes into account the iron losses and the dynamic equations for the PMSG currents are:

$$\frac{di_{md}}{dt} = \frac{1}{L_d} (v_d - R_{st} i_d + \omega L_q i_{mq}), \quad (5)$$

$$\frac{di_{mq}}{dt} = \frac{1}{L_d} (v_q - R_{st} i_q + \omega L_q i_{md} - \omega \psi_{PM}), \quad (6)$$

$$i_d = \frac{1}{R_c} (L_d \frac{di_{md}}{dt} - \omega L_q i_{mq} + R_c i_{md}), \quad (7)$$

$$i_q = \frac{1}{R_c} (L_q \frac{di_{mq}}{dt} + \omega L_d i_{md} + \omega \psi_{PM} + R_c i_{mq}), \quad (8)$$

$$i_{cd} = i_d - i_{md}, \quad (9)$$

$$i_{cq} = i_q - i_{mq}, \quad (10)$$

where i_d, i_q are the d_q axes currents, V_d, V_q are the d_q axes voltages, i'_{cd}, i'_{cq} are the d_q axes iron losses currents, i_{md}, i_{mq} are the d_q axes magnetizing currents, L_d, L_q are the d_q axes inductances, ψ_{PM} is the mutual flux due to magnets, ω is the fundamental frequency of the stator currents, R_c is the iron losses resistance and R_{st} is the stator resistance.

$$\text{The electromagnetic torque equation of the PMSG is: } T_e = \frac{2}{3} p [\psi_{PM} i_{mq} + (L_d - L_q) i_{md} i_{mq}] \quad (11)$$

where p is the number of pole pairs

2.3 Modeling of Batteries

The Battery block implements a basic dynamic model parameterized to be best common types of rechargeable batteries.

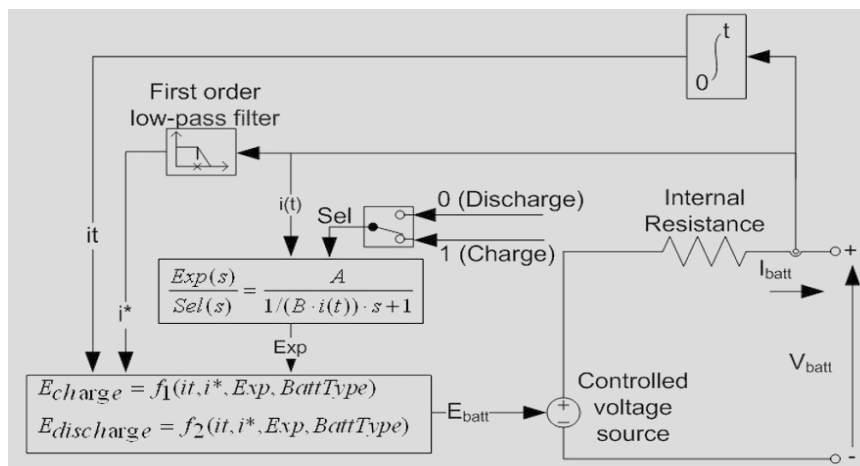


Fig. 2.4 Battery Equivalent Circuit of The Block Models

For the nickel-cadmium and nickel-metal-hydride battery types, the model uses these equations:

$$\text{Discharge Model } (i^* > 0) \quad f_1(i, i^*, i, \text{Exp}) = E_0 - K \cdot \frac{Q}{Q - i^*} \cdot i^* - K \cdot \frac{Q}{Q - i} \cdot i + \text{Laplace}^{-1} \left(\frac{\text{Exp}(s)}{\text{Sel}(s)} \cdot 0 \right)$$

$$\text{Charge Model } (i^* < 0) \quad f_2(i, i^*, i, \text{Exp}) = E_0 - K \cdot \frac{Q}{|i| + 0.1 \cdot Q} \cdot i^* - K \cdot \frac{Q}{Q - i} \cdot i + \text{Laplace}^{-1} \left(\frac{\text{Exp}(s)}{\text{Sel}(s)} \cdot \frac{1}{s} \right)$$

In the equations:

Here, E_{Batt} is nonlinear voltage, in V, E_0 is constant voltage, in V, $\text{Exp}(s)$ is exponential zone dynamics, in V, $\text{Sel}(s)$ represents the battery mode, $\text{Sel}(s) = 0$ during battery discharge, $\text{Sel}(s) = 1$ during battery charging, K is polarization constant, in Ah^{-1} , i^* is low frequency current dynamics, in A, i is battery current, in A.

it is extracted capacity, in Ah. Q is maximum battery capacity, in Ah., A is exponential voltage, in V., B is exponential capacity, in Ah^{-1} .

3. NOVEL OPTIMAL ENERGY MANAGEMENT (EM) CONTROLLER

The battery is controlled on the basis of their Energy Management capabilities. The bi-directional flow of battery needs buck-boost converter. The buck-boost converter has controlled via. PID controller. Fig. 3.23 show the block diagram of proposed Novel Optimal EM controller for the battery. Simulink model of EM controller shown in Fig. 3.1.

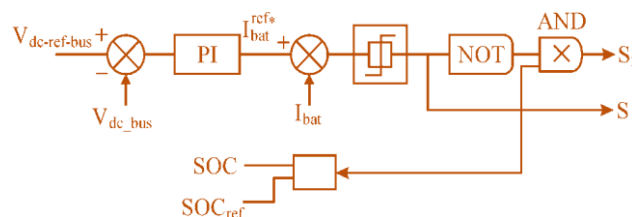


Fig. 3.1 Novel Optimal EM Controller for The Battery

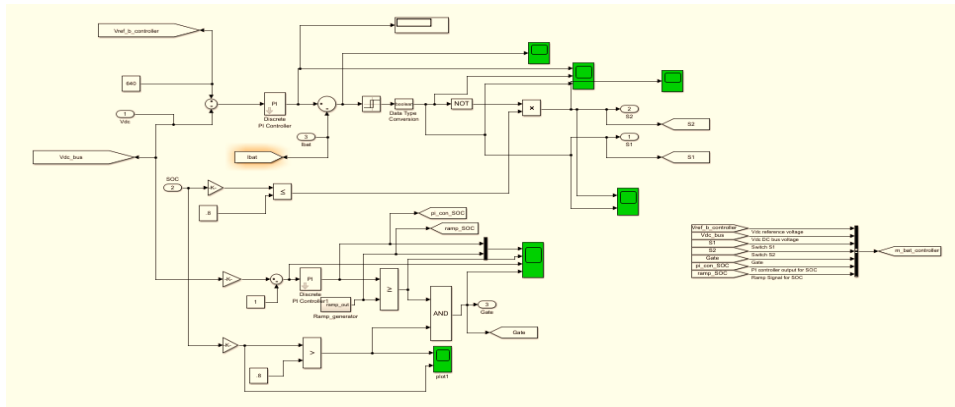


Fig. 3.2 Simulink model of Novel Optimal EM Controller

4. NOVEL OPTIMAL CONTROL STRATEGY FOR MICROGRID

The Artificial Neural Network (ANN) based control system is characterized by its rapid response, robustness, and stability. It holds the potential to enhance both the power quality and efficiency of microgrids. The proposed control strategy focuses on managing hybrid storage under two primary conditions: fluctuations in wind velocity and variations in solar irradiation. The block diagram illustrating the proposed ANN-based control strategy for hybrid storage management is presented in Figure 4.1.

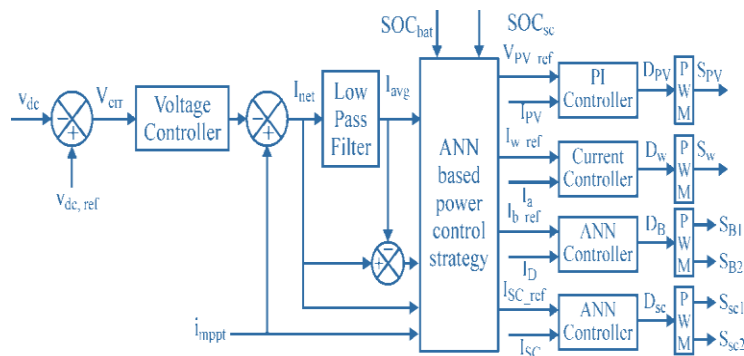
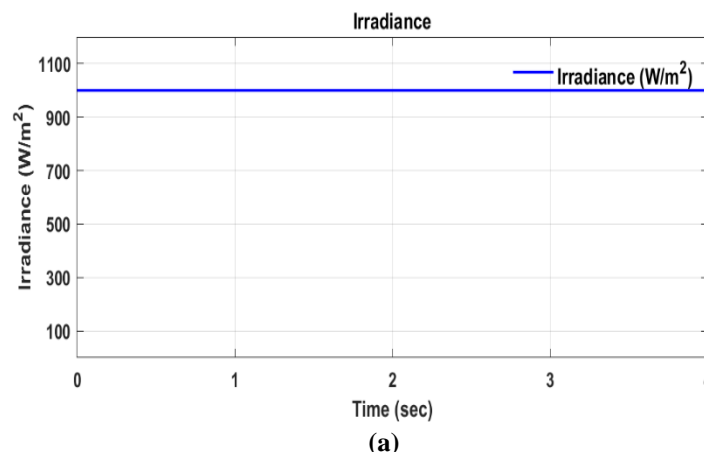


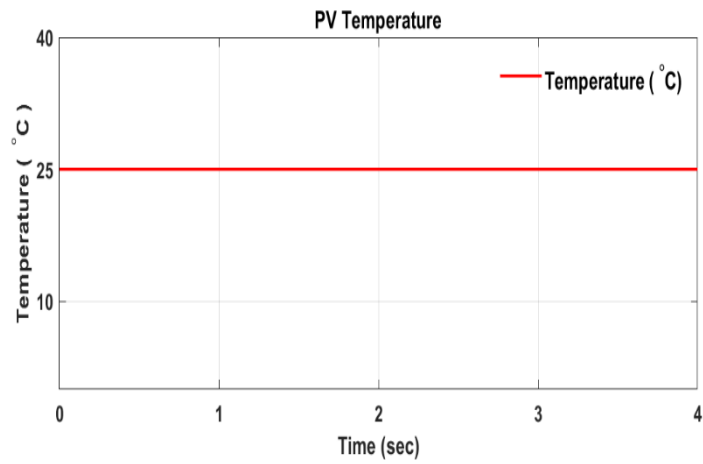
Fig. 4.1 Proposed Novel Optimal Control Strategy for Management of Hybrid Storage

5. SIMULATION RESULTS AND DISCUSSION

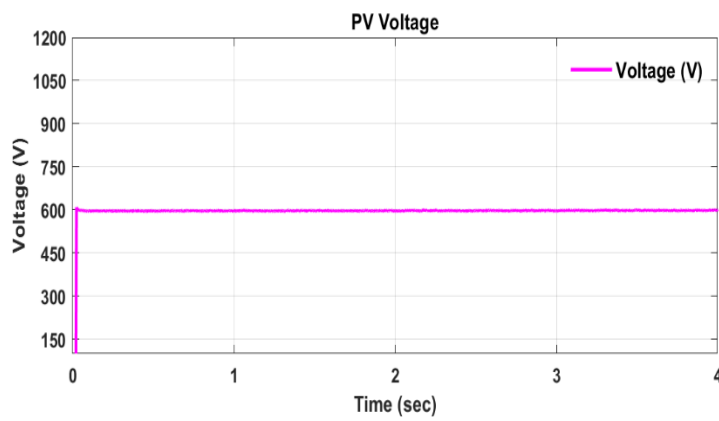
Case-1: Simulation Response at Constant Irradiance and Load with Successive Increase in Wind Speed

This case examines a scenario involving successive increases in wind speed in a stepped manner, transitioning from 8 m/s to 10 m/s, and further to 12 m/s, while maintaining a constant irradiance of 1000W/m² and a constant load. The simulation results are depicted below. Fig. 5.1 illustrates the simulation results for the PV system. Since the irradiance of the PV system remains constant, the power output of the system also remains constant at 9.9 kW, as shown in Fig. 5.1 (f). Additionally, Fig. 5.1 displays the parameters of Irradiance (W/m²), PV Temperature (°C), PV Voltage (volt), and PV output power (kW).

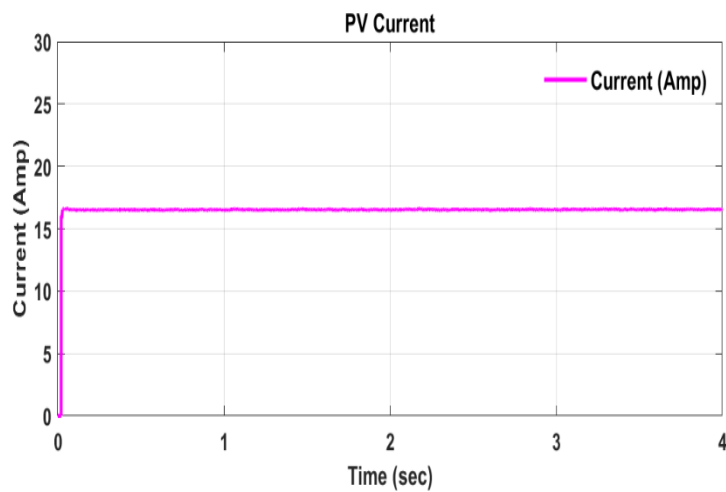




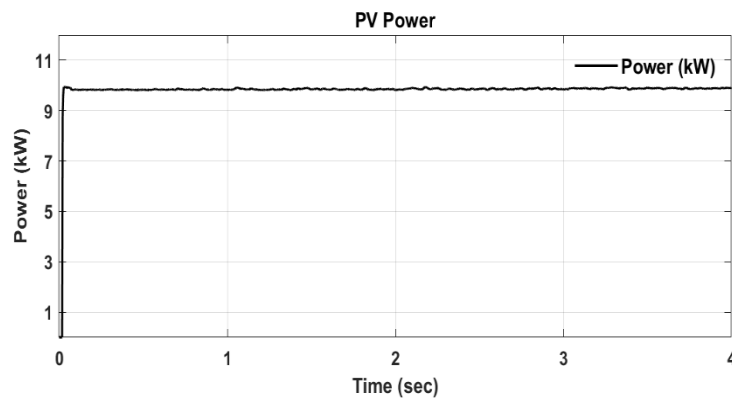
(b)



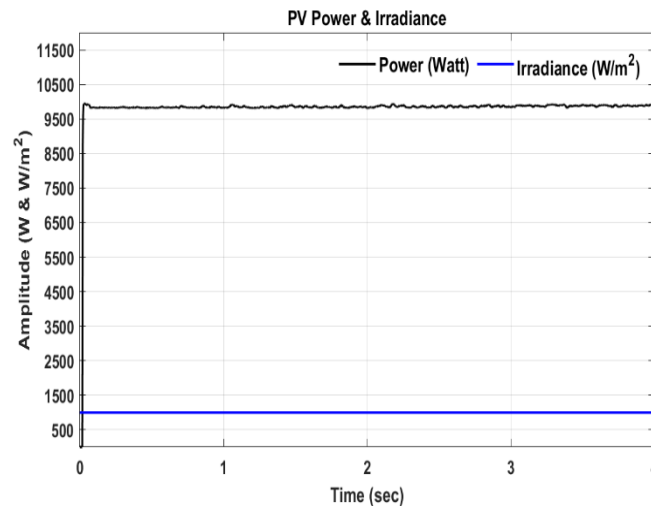
(c)



(d)



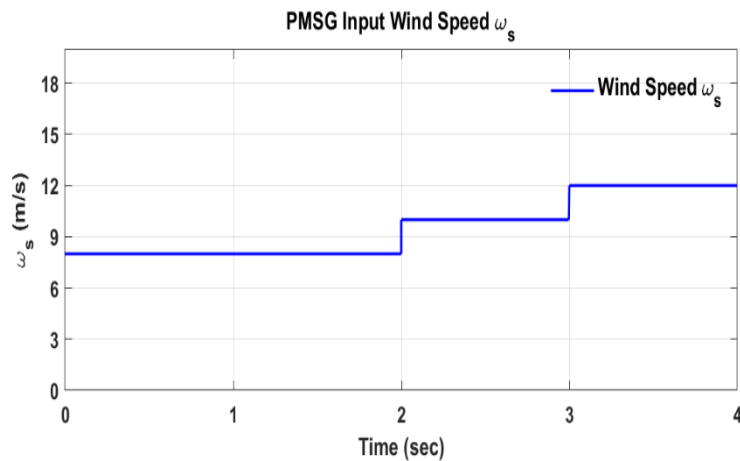
(e)



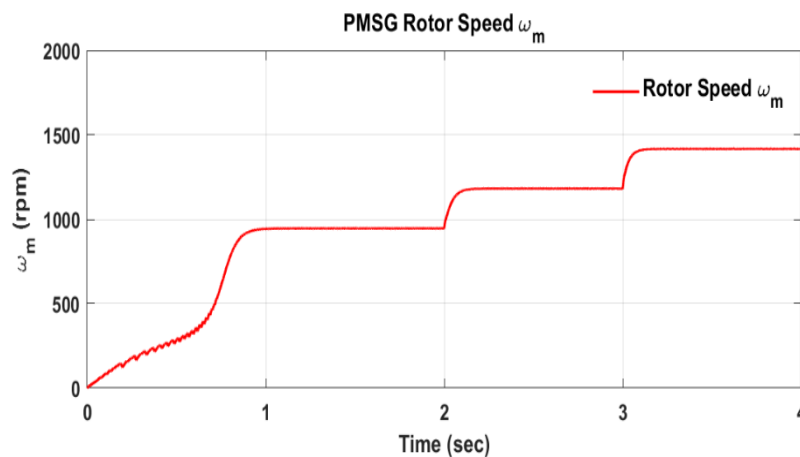
(f)

Fig. 5.1 (a) Waveform of Irradiance (W/m²), (b) PV Temperature (°C), (c) PV Voltage (volt), (d) PV Current (Amp), (e) PV output power(kW) and, (f) PV output power(W) with irradiance

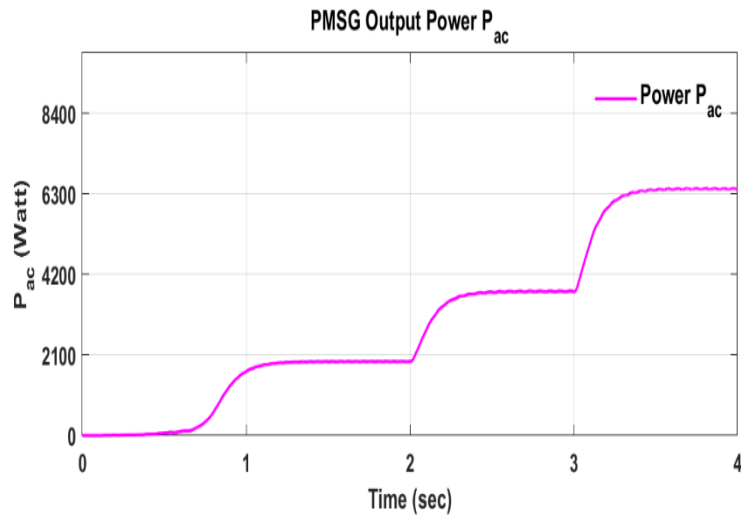
Fig. 5.2 presents various parameters including input wind speed ω_s , Permanent Magnet Synchronous Generator (PMSG) speed ω_m , PMSG output power P_{ac} , electromagnetic torque T_e , mechanical torque T_m , PMSG phase to phase voltages V_{ab} , V_{bc} , V_{ca} , and PMSG phase current I_a , I_b , I_c . Observing the results, at an input wind speed of 8 m/s, the PMSG speed is 950 rpm, resulting in a power output of 1930 watts. At $t=2$ sec, when the input wind speed increases from 8 m/s to 10 m/s and the PMSG speed increases to 1200 rpm, the power output also rises to 3750 watts. Similarly, at $t=4$ sec, when the input wind speed further increases from 10 m/s to 12 m/s and the PMSG speed increases to 1415 rpm, the power output further increases to 6300 watts, as depicted in Fig. 5.2.



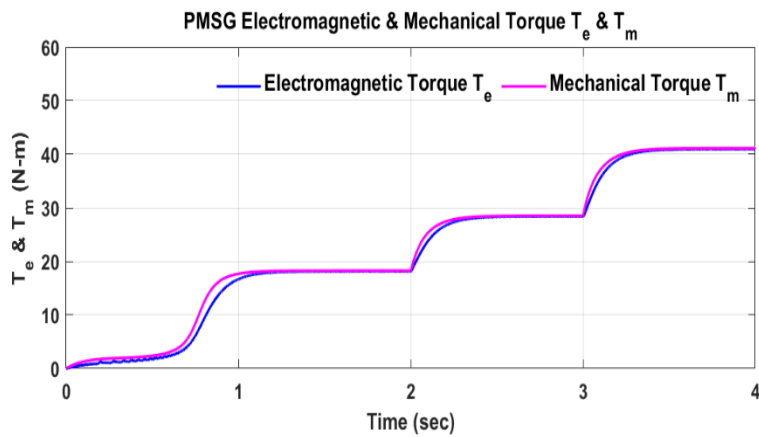
(a)



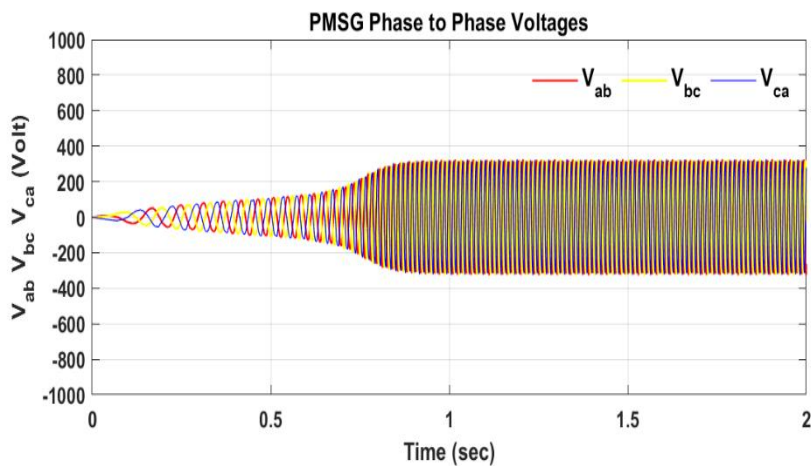
(b)



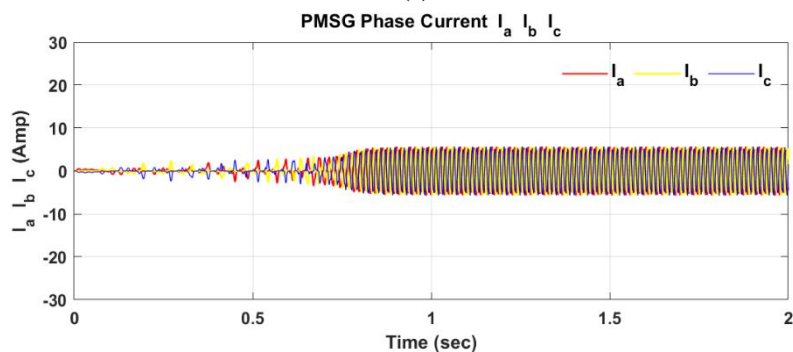
(c)



(d)



(e)



(f)

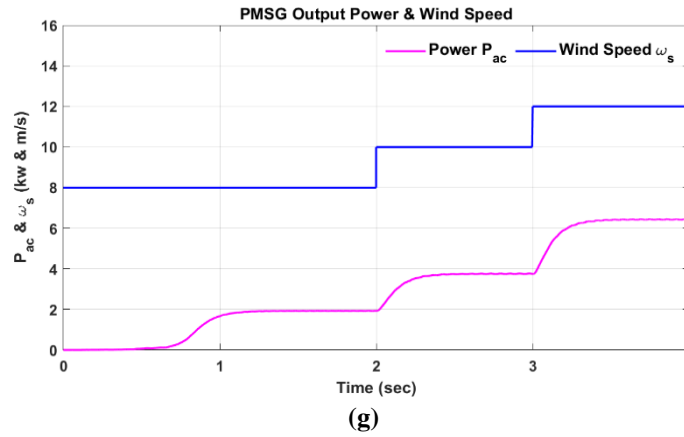


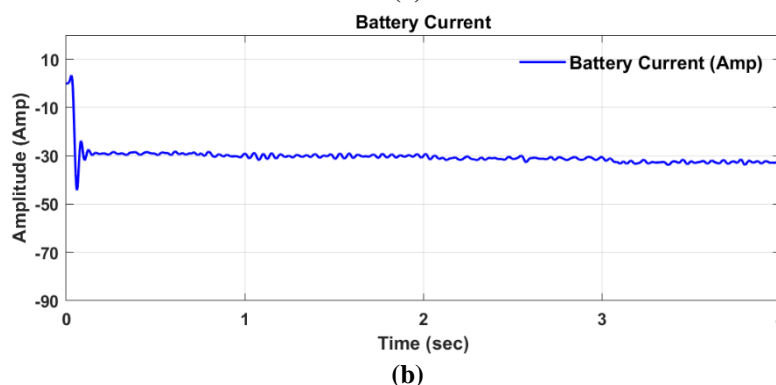
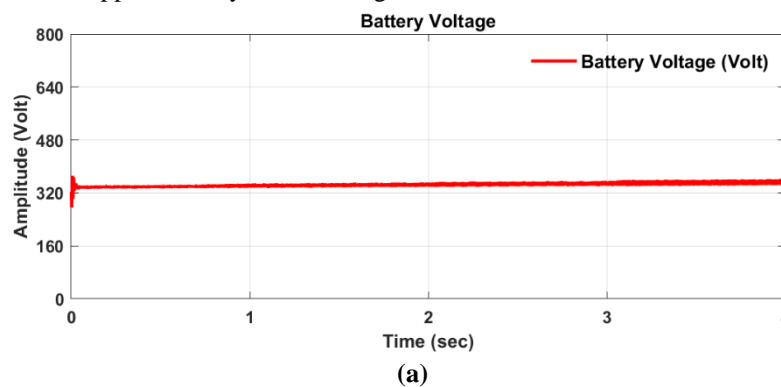
Fig. 5.2 Waveform of, (a) input wind speed ω_s , (b) PMSG speed ω_m , (c) PMSG output power P_{ac} , (d) Electromagnetic & mechanical torque T_e & T_m , (e) PMSG phase to phase voltages V_{ab} V_{bc} V_{ca} , (f) PMSG phase current I_a I_b I_c and, (g) PMSG output power with wind speed

The output from both the Photovoltaic (PV) system and the Wind Energy Conversion System (WECS) is directed to a common DC link bus. Integrated at this same DC link bus is a battery storage system, facilitated by an intermediate DC-DC Buck-Boost converter. Within the control algorithm, Fuzzy Logic Control (FLC) is utilized to effectively manage the power of the hybrid system alongside the battery storage system.

Fig. 5.2 illustrates the simulation results for the battery storage system, showcasing the battery voltage, battery current, and battery State of Charge (SOC). As depicted in Fig. 11(a), the battery voltage remains constant at 340V throughout the simulation. The initial SOC of the battery is set at 60% at the beginning of the simulation.

Given that the load demand does not exceed the generated power, the surplus generated power is channeled to the battery via the DC-DC converter. As observed in Fig. 5.3 (b), when the WECS operates at 8 m/s and the PV system at 1000 W/m² initially, the current supplied to the battery is approximately 16A. Consequently, as the battery receives current from the hybrid system, it commences charging, leading to an increase in SOC, as depicted in Fig. 5.3(c).

At $t=2$ sec, when the power output from the WECS system increases due to an increase in input wind speed from 8 m/s to 10 m/s, the current supplied to the battery also increases from 16A to 21A. Consequently, the rate of SOC increase also accelerates. Similarly, at $t=4$ sec, with the input wind speed increasing to 12 m/s, the current supplied to the battery increases to approximately 27A, leading to a further acceleration in the rate of SOC increase.



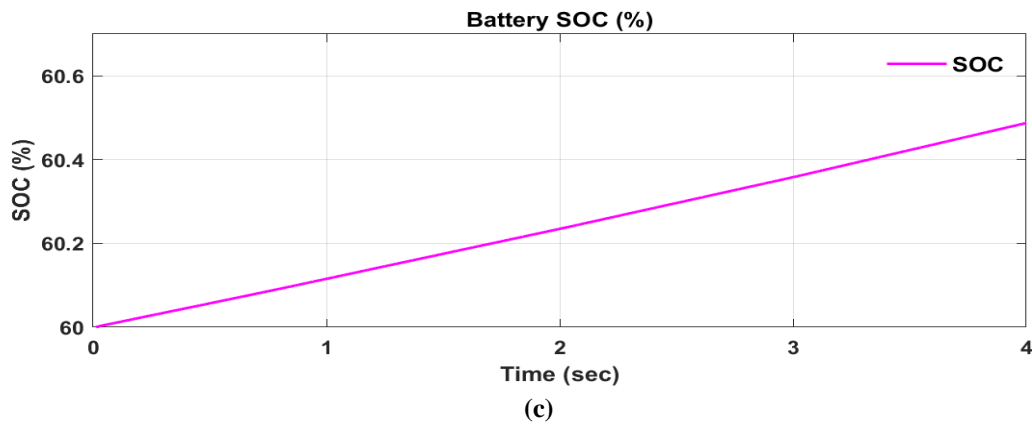


Fig. 5.3 Waveform of (a) Battery Output Voltage (volt), (b) Battery Output Current (Amp), (c) Battery SOC (%)

Fig. 5.4(b) illustrates the simulation results of the DC bus reference voltage alongside the actual DC bus voltage, as well as the switching pulses for switches S1 and S2 of the DC-DC buck-boost converter, and the controller output. The figure demonstrates that the control strategy effectively maintains a constant DC bus voltage throughout the simulation.

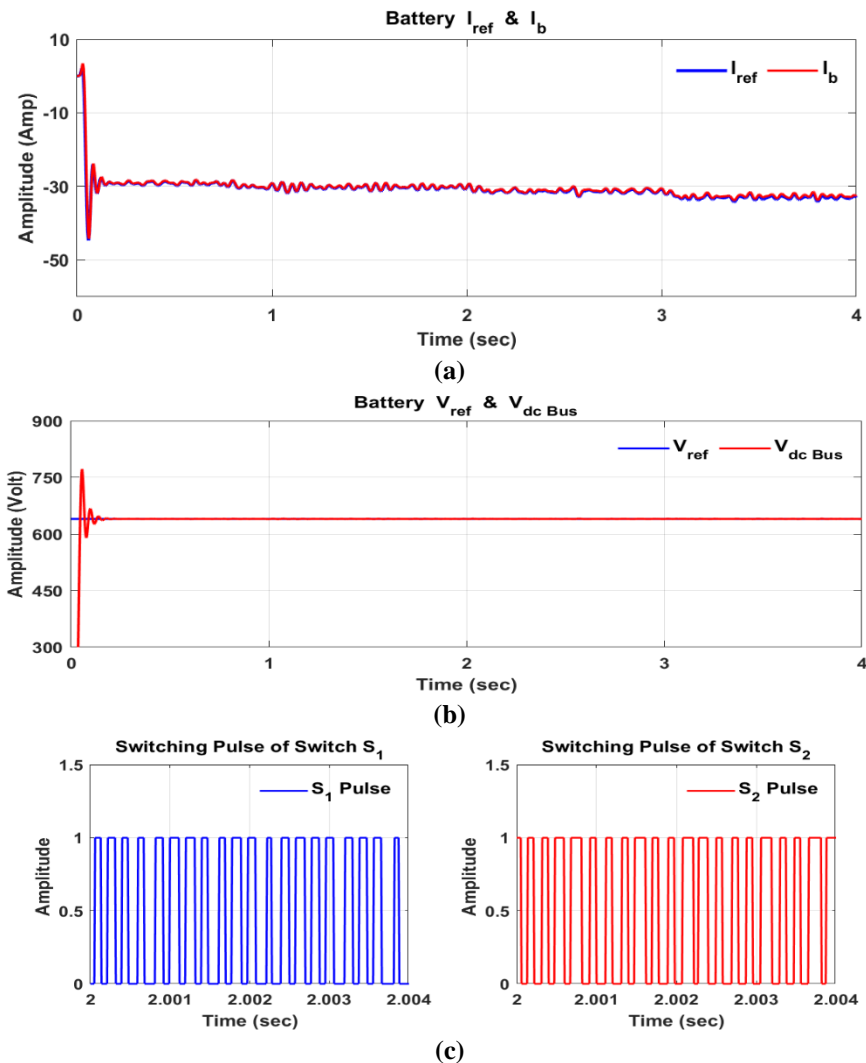


Fig. 5.4 Waveform of (a) Battery current with reference current, (b) Reference voltage with dc bus voltage and, (c) Switching pulses of switch S₁ & S₂

The generated DC bus voltage is supplied to the multilevel inverter. A fuzzy logic controller regulates the inverter's AC output voltage, which is then directed to the load. Fig. 5.5 displays the output voltage of the multilevel inverter, showcasing the controlled AC voltage. Additionally, Fig. 5.5 illustrates the switching pulses of the inverter.

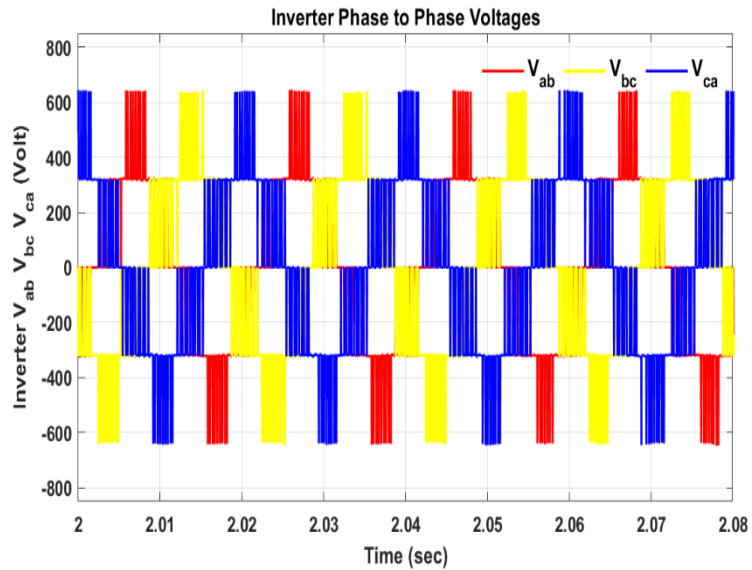
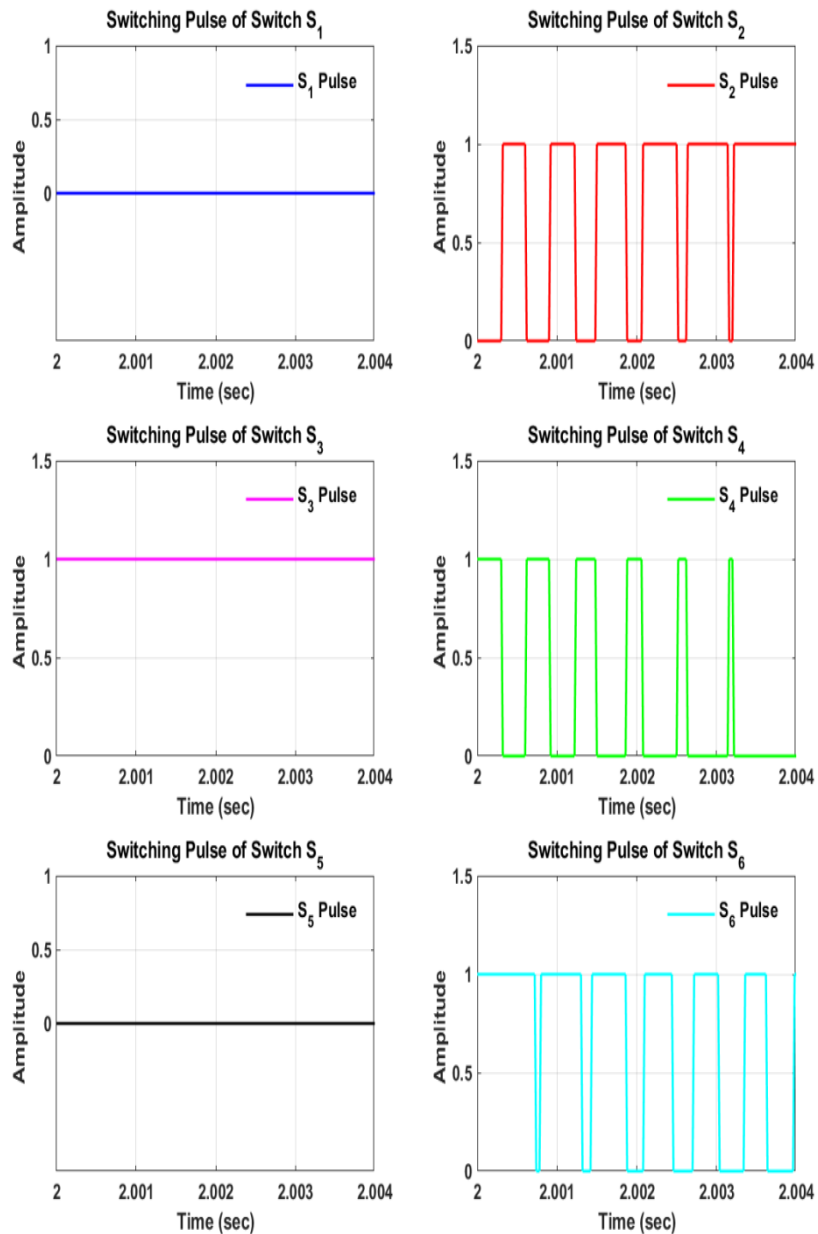


Fig. 5.5 Multilevel Inverter Output Phase to Phase Voltages V_{ab} , V_{bc} , V_{ca}



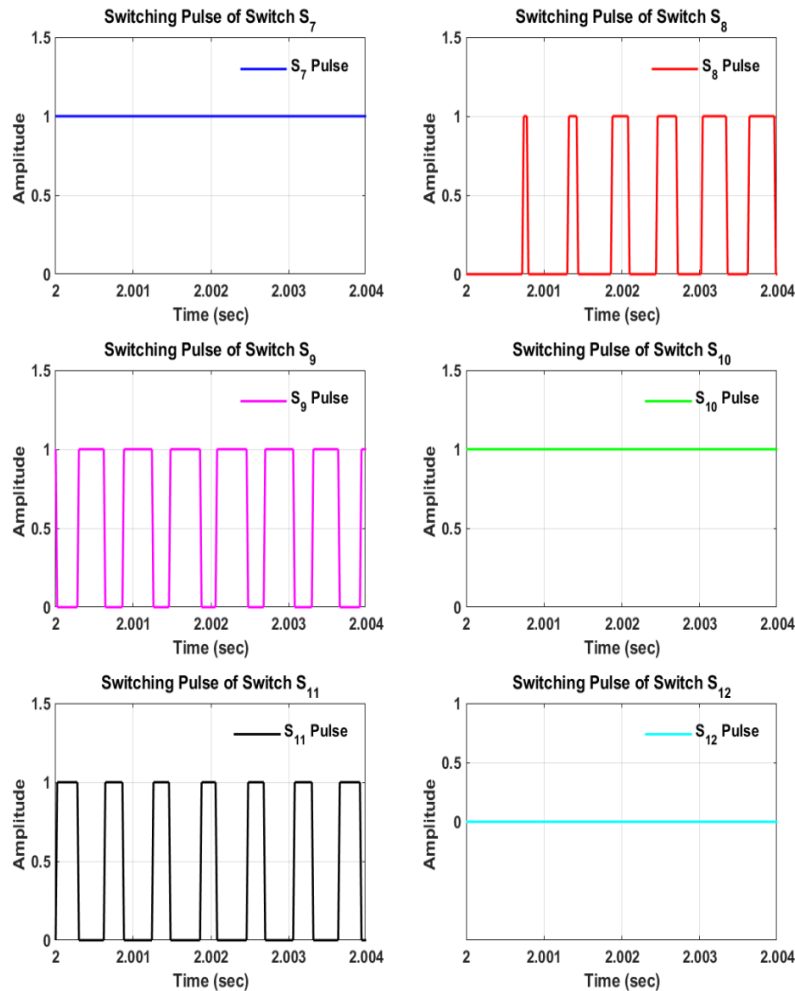


Fig. 5.6 Switching Pulses Waveform of Inverter Switches

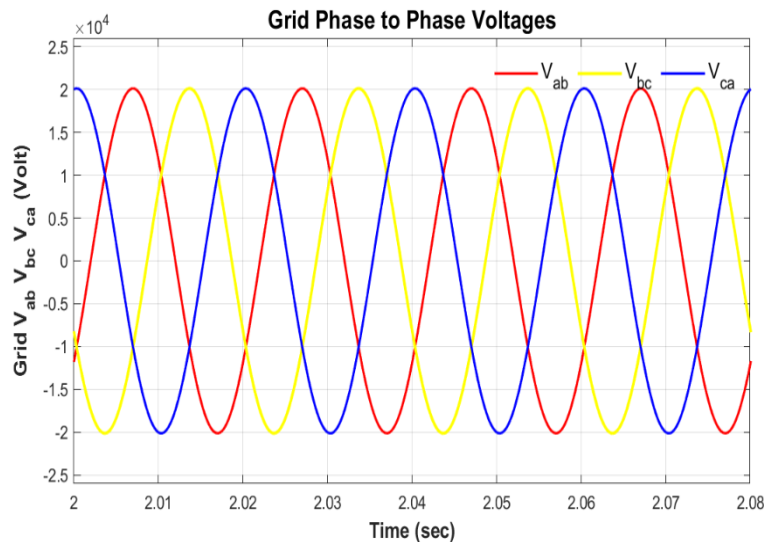


Fig. 5.7 Simulation Results for Grid, Waveform of Phase-Phase Voltage

In this scenario, a comparison of load demand, battery system, Wind Energy Conversion System (WECS), and Photovoltaic (PV) system power is presented in Fig. 5.8. The load is maintained at a constant level, and the PV irradiance remains constant, resulting in a steady PV power output. However, during this simulation, wind speed varies in a stepped manner, causing fluctuations in the power output of the WECS system.

As observed from the results, at $t=2$ sec, the power output of the WECS system increases, leading to a corresponding increase in the power fed to the battery. Similarly, at $t=3$ sec, the power output further increases as wind speed rises, resulting in an increased power fed to the battery.

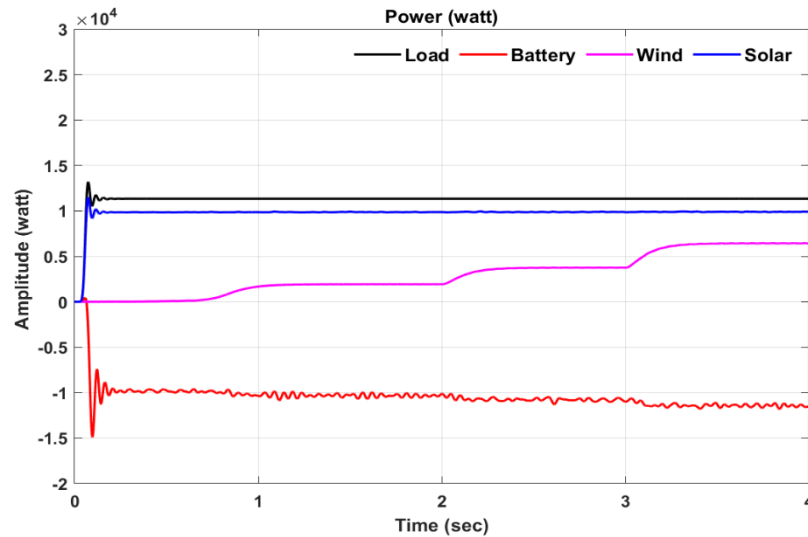


Fig. 5.8 Power Levels of Load, Battery, Wind and Solar System

CONCLUSION

The proposed Solar PV- wind system is also developed for validation of the simulation results. The source-side converters possess the capability to extract optimal power from individual sources, facilitating voltage conversion and full control of PV/WECS/Battery current and DC bus voltage. The DC bus voltage is maintained at nearly constant values. Load-side multilevel inverters are adept at maintaining a constant output voltage across the load, even under dynamic load conditions. Output power is effectively controlled according to load demands. The hybrid solar PV-wind system demonstrates efficient, stable, reliable, and continuous operation in isolated mode. Results indicate that the developed control strategy efficiently distributes the load demand among different individual sources.

REFERENCES

- [1] Ahmed Aghmadi; Hossam Hussein; Osama A. Mohammed 2023. "Enhancing Energy Management System for a Hybrid Wind Solar Battery Based Standalone Microgrid" IEEE International Conference on Environment and Electrical Engineering held during 06-09 June 2023, pp. 1-6.
- [2] P. Sai Sampath Kumar et al. 2023. "Energy Management System for Small Scale Hybrid Wind Solar Battery Based Microgrid" 4th International Conference on Design and Manufacturing Aspects for Sustainable Energy (ICMED-ICMPC 2023).
- [3] Imran Shafi; Harris Khan; Muhammad Siddique Farooq; Isabel de la Torre Diez; Yini Miró; Juan Castanedo Galán and Imran Ashraf 2023. "An Artificial Neural Network-Based Approach for Real-Time Hybrid Wind-Solar Resource Assessment and Power Estimation" Energies, Vol.16, issues no. 10, 2023.
- [4] Satyajeet Sahoo et al. 2022. "Artificial Deep Neural Network in Hybrid PV System for Controlling the Power Management" Hindawi International Journal of Photoenergy, Vol.10, issues no. 02, 2022.
- [5] Arul, P.G., Ramachandaramurthy, V.K. and Rajkumar, R. K., "Control strategies for a hybrid renewable energy system: A Review," Renewable and Sustainable Energy Reviews, vol. 42, pp. 597-608, 2015.
- [6] Lazarov, V., Notton, G., Zarkov, Z. and Bochev, I. "Hybrid power systems with renewable energy sources types, structures, trends for research and development," In: Proceedings of 11th International conference on electrical machines, drives and power systems, held at Bulgaria during September 15-16, 2005, pp.515-520.
- [7] Siddaiah, R. and Saini, R.P., "A review on planning, configurations, modeling and optimization techniques of hybrid renewable energy systems for off grid applications," Renewable and Sustainable Energy Reviews vol. 58, pp. 376-396, 2016.
- [8] Chauhan, A. and Saini, R.P., "A review on Integrated Renewable Energy System based power generation for stand-alone applications: Configurations, storage options, sizing methodologies and control," Renewable and Sustainable Energy Reviews vol. 38, pp. 99-120, 2014.
- [9] Nehrir, M. H., Wang, C., Strunz, H. Aki, Ramakumar, R., Bing, J., Miao, Z. and Salameh, "A review of hybrid renewable/alternative energy systems for electric power generation: configurations, control, and applications," IEEE Transactions on Sustainable Energy vol. 2, no.1, pp. 392-403, 2011.
- [10] Wang, C. and Nehrir, M. H., "Power management of a stand-alone wind/photovoltaic/ fuel cell energy

- system,” IEEE Transactions on energy conversion vol. 23, no. 5, pp. 957-967, 2008.
- [11] M. Aarif; D. Joshi; R. Jangid and S.S. Sharma, “Grid Power Smoothing Management for Direct Drive PMSG Variable Speed Wind Energy Conversion System with Multilevel Converter”, IEEE 7th International Conference on ICT for Sustainable Development, Organized by Global Knowledge Foundation during 29-30, July 2022 at Goa, India.
- [12] Y. Joshi; J.k Maherchandani; V.K Yadav; R. Jangid; S. Vyas and S.S Sharma, “Performance Improvement of Standalone Battery Integrated Hybrid System” IEEE 7th International Conference on Electrical Energy Systems (ICEES), Organized by Sri Sivasubramaniya Nadar College of Engineering during 11-13 Feb. 2021 at Chennai, India.
- [13] R. Jangid; J.k Maherchandani; R.R. Joshi and B.D Vairagi, “Development of Advance Energy Management Strategy for Standalone Hybrid Wind & PV System Considering Rural Application”, IEEE 2nd International Conference on Smart Systems and Inventive Technology, Organized by Francis Xavier Engineering College during November 27-29, 2019 at Tirunelveli, India.
- [14] R. Jangid; K. Parikh and P. Anjana, “Reducing the Voltage Sag and Swell Problem in Distribution System Using Dynamic Voltage Restorer with PI Controller”, International Journal of Soft Computing and Engineering, ISSN: 2231-2307, Vol.-3, Issue-6, January 2014.
- [15] R. Jangid; J.k Maherchandani; V.K Yadav and R.K Swami, “Energy Management of Standalone Hybrid Wind-PV System”, Journal of Intelligent Renewable Energy Systems (John Wiley & Sons, Inc.) Pages 179-198, 2022.
- [16] H. Kumawat and R. Jangid, “Using AI Techniques to Improve the Power Quality of Standalone Hybrid Renewable Energy Systems”, Crafting a Sustainable Future Through Education and Sustainable Development, IGI Global, Pages 219-228, 2023.
- [17] H. Kumawat; R. Jangid, “Performance and Investigation of Two Drive Train Interfaced Permanent Magnet Synchronous Generator for Wind Energy Conversion System”, Journal of Emerging Technologies and Innovative Research, ISSN:2349-5162, Volume 7, Issue 1, January 2020.
- [18] R. Jangid et. al., “Smart Household Demand Response Scheduling with Renewable Energy Resources”, IEEE Third International Conference on Intelligent Computing and Control System, Organized by Vaigai College of Engineering during May 15-17, 2019 at Madurai, India.
- [19] S. Kumar; R. Jangid and K. Parikh “Comparative Performance Analysis of Adaptive Neuro-Fuzzy Inference System (ANFIS) & ANN Algorithms Based MPPT Energy Harvesting in Solar PV System.” International Journal of Technical Research and Science, vol. 8, Issue 3, March 2023.
- [20] S. Sharma; R. Jangid and K. Parikh “Development of Intelligent Control Strategy for Power Quality Improvement of Hybrid RES Using AI Technique” International Journal of Technical Research and Science, vol. VIII, Issue II, Feb. 2023.
- [21] L. Jhala et al., “Development of Control Strategy for Power Management in Hybrid Renewable Energy System” International Journal of Technical Research and Science, vol. VI, Issue XII, Dec. 2021.
- [22] Mohod, S.W. and Aware, M.V., “A STATCOM-control scheme for grid connected wind energy system for power quality improvement,” IEEE Systems Journal vol. 4, no. 2, pp. 346-352, 2010.
- [23] Frangieh, W. and Najjar, M. B., “Active control for power quality improvement in hybrid power systems,” In: Proceedings of IEEE 3rd International Conference on Technological Advances in Electrical, Electronics and Computer Engineering held at Lebanon during April 29-30, 2015, pp. 218-223.
- [24] Rini, T. H. and Razzak, M. A., “Voltage and power regulation in a solar-wind hybrid energy system,” In: Proceedings of IEEE International WIE Conference on Electrical and Computer held at Dhaka during December 19-20, 2015, pp. 231-234.